

Kinetic Studies on the Reductive Elimination of *cis*-PtMe(SiPh₃)(PMe₂Ph)₂ and *cis*-PtMe(GePh₃)(PMe₂Ph)₂. The First Comparison between C–Si and C–Ge Reductive Elimination

Fumiyuki Ozawa,* Toshihiko Hikida, Koh Hasebe, and Takuya Mori

Department of Applied Chemistry, Faculty of Engineering, Osaka City University, Sumiyoshi-ku, Osaka 558, Japan

Received September 25, 1997

The novel complex *cis*-PtMe(GePh₃)(PMe₂Ph)₂ (**2b**) was prepared by the treatment of *trans*-PtCl(GePh₃)(PMe₂Ph)₂ (**3**) with 2 equiv of MeLi in THF followed by methanolysis of the reaction system. The X-ray and NMR data of **2b**, together with the NMR data of related *cis*-PtMe(SiPh₃)(PMe₂Ph)₂ (**1b**) and *cis*-PtMe₂(PMe₂Ph)₂ (**4**), indicated the following order of trans influence: SiPh₃ >> GePh₃ > Me. While the trans influence of the GePh₃ ligand is much lower than that of the SiPh₃ ligand and only slightly higher than that of the Me ligand, the GePh₃ ligand was found to possess a much higher trans effect than the methyl ligand, comparable to the SiPh₃ ligand. Thermolysis of **1b** and **2b** in toluene-*d*₈ in the presence of an excess amount of diphenylacetylene provided quantitative yields of reductive-elimination products MeSiPh₃ and MeGePh₃, respectively. Kinetic studies revealed that the methyl-germyl complex **2b** is much more stable than the methyl-silyl complex **1b**. The reductive elimination proceeds for both complexes via a process involving a prior ligand displacement of one of the PMe₂Ph ligands with diphenylacetylene, followed by elimination of MeSiPh₃ or MeGePh₃ from the resulting acetylene-coordinated species. Factors governing the reactivity of C–Si and C–Ge reductive elimination from a Pt(II) center are discussed.

Introduction

Reductive elimination of organotransition-metal complexes is a crucial process in catalytic reactions.¹ In the past decade, a great deal of research has been carried out to elucidate the mechanism and kinetics of the reductive elimination that provides a carbon–carbon or a carbon–hydrogen bond.² In contrast, studies of the reductive elimination that causes carbon–heteroatom bond formation are still limited and their mechanistic details remain to be explored.^{3–5} Recently, Hartwig and co-workers examined the mechanisms of reductive

elimination of aryl(amido)- and aryl(thiolato)palladium complexes.^{3b,d} On the other hand, we reported a kinetic study on the reductive elimination of *cis*-PtMe(SiPh₃)(PMePh₂)₂ to give MeSiPh₃ and a platinum(0) species.⁴ This type of reaction, which forms a carbon–silicon bond, has been assumed as the product-forming step in many catalytic silylation reactions of organic molecules,⁶ while definitive examples of C–Si reductive elimination are rare⁵ and their mechanisms have been investigated only for a few instances.^{5a,b}

We have found that the reductive elimination of *cis*-PtMe(SiPh₃)(PMePh₂)₂ (**1a**) readily proceeds even at room temperature.⁴ The reactivity observed was unexpectedly high as compared with that of common diorganoplatinum(II) complexes such as *cis*-PtMe₂(PMePh₂)₂, which is thermally inactive toward reductive elimination.⁷ Since theoretical and thermochemical data have indicated that the Pt–Si bond is generally

(1) Parshall, G. W.; Ittel, S. D. *Homogeneous Catalysis*; Wiley-Interscience: New York, 1992.

(2) (a) Brown, J. M.; Cooley, N. A. *Chem. Rev. (Washington, D.C.)* **1988**, *88*, 1031. (b) Yamamoto, A. *Organotransition Metal Chemistry, Fundamental Concepts and Applications*; Wiley-Interscience: New York, 1986. (c) Collman, J. P.; Hegedus, L. S.; Norton, J. R.; Finke, R. G. *Principles and Applications of Organotransition Metal Chemistry*; University Science Books: Mill Valley, CA, 1987.

(3) For recent examples of reductive elimination giving a carbon–heteroatom bond other than the carbon–silicon bond, see: (a) Villanueva, L. A.; Abboud, K. A.; Boncella, J. M. *Organometallics* **1994**, *13*, 3921. (b) Driver, M. S.; Hartwig, J. F. *J. Am. Chem. Soc.* **1995**, *117*, 4708. (c) Hartwig, J. F.; Richards, S.; Barañano, D.; Paul, F. *J. Am. Chem. Soc.* **1996**, *118*, 3626. (d) Barañano, D.; Hartwig, J. F. *J. Am. Chem. Soc.* **1995**, *117*, 2937. (e) Han, R.; Hillhouse, G. L. *J. Am. Chem. Soc.* **1997**, *119*, 8135. (f) Koo, K.; Hillhouse, G. L. *Organometallics* **1996**, *15*, 2669. (g) Fryzuk, M. D.; Joshi, K.; Chadha, R. K.; Rettig, S. J. *J. Am. Chem. Soc.* **1991**, *113*, 8724. (h) Han, L.; Choi, N.; Tanaka, M. *Organometallics* **1996**, *15*, 3259. (i) Nakazawa, H.; Matsuoka, Y.; Nakagawa, I.; Miyoshi, K. *Organometallics* **1992**, *11*, 1385. (j) Komiya, S.; Akai, Y.; Tanaka, K.; Yamamoto, T.; Yamamoto, A. *Organometallics* **1985**, *4*, 1130. (k) Thompson, J. S.; Randall, S. L.; Atwood, J. L. *Organometallics* **1991**, *10*, 3906.

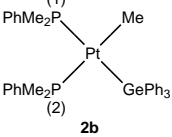
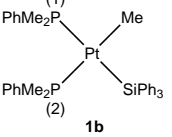
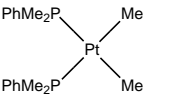
(4) Ozawa, F.; Hikida, T.; Hayashi, T. *J. Am. Chem. Soc.* **1994**, *116*, 2844.

(5) (a) Tanaka, Y.; Yamashita, H.; Shimada, S.; Tanaka, M. *Organometallics* **1997**, *16*, 3246. (b) Aizenberg, M.; Milstein, D. *J. Am. Chem. Soc.* **1995**, *117*, 6456. (c) Akita, M.; Hua, R.; Oku, T.; Tanaka, M.; Moro-oka, Y. *Organometallics* **1996**, *15*, 4162. (d) Okazaki, M.; Tobita, H.; Ogino, H. *Organometallics* **1996**, *15*, 2790. (e) Mitchell, G. P.; Tilley, T. D. *Organometallics* **1996**, *15*, 3477. (f) Schubert, U. *Angew. Chem., Int. Ed. Engl.* **1994**, *33*, 419. (g) Lin, W.; Wilson, S. R.; Girolami, G. S. *Organometallics* **1994**, *13*, 2309. (h) Schubert, U.; Müller, C. *J. Organomet. Chem.* **1989**, *373*, 165. (i) Brinkman, K. C.; Blakeney, A. J.; Krone-Schmidt, W.; Gladysz, J. A. *Organometallics* **1984**, *3*, 1325.

(6) (a) Brunstein, P.; Knorr, M. *J. Organomet. Chem.* **1995**, *500*, 21. (b) Recatto, C. A. *Aldrichimica Acta* **1995**, *28*, 85. (c) Tilley, T. D. In *The Chemistry of Organic Silicon Compounds*; Patai, S., Rappoport, Z., Eds.; Wiley: Chichester, U.K., 1989; p 1415.

(7) Low, J. J.; Goddard, W. A., III. *J. Am. Chem. Soc.* **1986**, *108*, 6115 and references therein.

Table 1. Characteristic NMR Data for **1b**, **2b**, and **4a**

complex	$^{31}\text{P}\{^1\text{H}\}$ NMR	$^{13}\text{C}\{^1\text{H}\}$ NMR
 <p>2b</p>	P(1): δ -4.6, $^2J_{\text{P-P}} = 19$ Hz, $^1J_{\text{Pt-P}} = 1955$ Hz P(2): δ -12.2 (d), $^2J_{\text{P-P}} = 19$ Hz, $^1J_{\text{Pt-P}} = 1972$ Hz	PtMe: δ -0.37 (dd), $^2J_{\text{P-C}} = 83$ and 7 Hz, $^1J_{\text{Pt-C}} = 486$ Hz
 <p>1b</p>	P(1): δ , -3.7 (d), $^2J_{\text{P-P}} = 19$ Hz, $^1J_{\text{Pt-P}} = 1330$ Hz, $^2J_{\text{Si-P}} = 198$ Hz P(2): δ -10.9 (d), $^2J_{\text{P-P}} = 19$ Hz, $^1J_{\text{Pt-P}} = 2048$ Hz	PtMe: δ 1.3 (dd), $^2J_{\text{P-C}} = 81$ and 8 Hz, $^1J_{\text{Pt-C}} = 508$ Hz
 <p>4</p>	$\delta = 10.1$ (s), $^1J_{\text{Pt-P}} = 1844$ Hz	PtMe: δ 2.9 (AXX'), $^1J_{\text{Pt-C}} = 589$ Hz

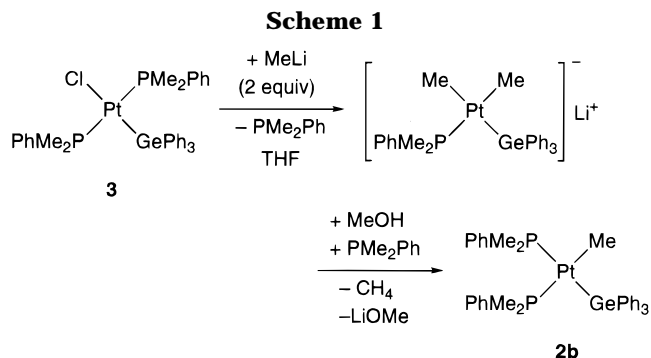
^a In CD₂Cl₂, at -20 °C. Complete NMR data for **2b** are reported in the Experimental Section.

much stronger than the Pt–C bond and the C–Si bond is weaker than the C–C bond,⁸ the much higher reactivity of methyl(silyl)platinum compared to that of dimethylplatinum is attributed to kinetic factors, probably reflecting the size of the silicon atom being greater than that of the carbon atom, which facilitates orbital interaction between silicon and carbon at the transition state, and the low electronegativity of silicon, which reduces the energy barrier attendant on the reduction of platinum(II) to platinum(0) during the reductive-elimination process. To obtain further information on the C–Si reductive elimination, we compared in this study the reactivities of methyl(silyl)platinum and the related methyl(germyl)platinum species. Kinetic studies revealed the germyl complex to be much less reactive than the silyl complex toward reductive elimination.

Results and Discussion

Preparation of Methyl(germyl)platinum(II). To compare the C–Si and C–Ge reductive-elimination reactions, *cis*-PtMe(EPh₃)L₂ (E = Si, Ge) complexes having the same tertiary phosphine ligand (L) are needed. Since the silyl derivatives have already been prepared,^{4,9} syntheses of the germyl analogues were examined in this study.

First of all, we tried to synthesize *cis*-PtMe(GePh₃)(PMePh₂)₂ (**2a**), which is the germyl analogue of *cis*-PtMe(SiPh₃)(PMePh₂)₂ (**1a**) employed in the previous study of reductive elimination.⁴ Treatment of *trans*-PtCl(GePh₃)(PMePh₂)₂ with 2 equiv of MeLi in THF followed by methanolysis of the resulting solution, however, did not form **2a** but instead provided a platinum(II) complex having a *trans* geometry: $^{31}\text{P}\{^1\text{H}\}$ NMR δ 6.9 (s, $^1J_{\text{Pt-P}} = 2769$ Hz). This result differs from the synthetic reaction of **1a**, in which the treat-



ment of *trans*-PtCl(SiPh₃)(PMePh₂)₂ with an excess amount of MeLi gives the platinate complex Li⁺[PtMe₂(SiPh₃)(PMePh₂)₂][−] with liberation of 1 equiv of PMePh₂. Methanolysis of the reaction system leads to the selective formation of **1a**.

On the other hand, a *cis*-methyl(germyl)platinum compound bearing two PMe₂Ph ligands (**2b**) could be prepared in good yield, starting from *trans*-PtCl(GePh₃)(PMe₂Ph)₂ (**3**) (Scheme 1). The reaction was examined by $^{31}\text{P}\{^1\text{H}\}$ NMR spectroscopy. When 2 equiv of MeLi was added to a THF solution of **3** at room temperature, the signal of **3** at δ -5.6 (s, $^1J_{\text{Pt-P}} = 2667$ Hz) instantly disappeared, and a singlet at δ -9.7 ($^1J_{\text{Pt-P}} = 2028$ Hz) assignable to Li⁺[PtMe₂(GePh₃)(PMe₂Ph)][−] and a broad signal arising from free PMe₂Ph (δ -44.8) appeared in a 1:1 ratio. Addition of an excess amount of methanol to the system at -20 °C led to the formation of *cis*-PtMe(GePh₃)(PMe₂Ph)₂ (**2b**) with 93% selectivity, which was isolated in 65% yield by recrystallization from CH₂Cl₂–Et₂O.

Table 1 summarizes the characteristic NMR data for **2b**. Also listed are the data for the related complexes *cis*-PtMe(SiPh₃)(PMe₂Ph)₂ (**1b**)⁹ and *cis*-PtMe₂(PMe₂Ph)₂ (**4**). The $^{31}\text{P}\{^1\text{H}\}$ NMR spectrum of **2b** exhibited two sets of doublets at δ -12.2 and -4.6. Since the doublet at δ -12.2 was observed in a region similar to that for the signals arising from the PMe₂Ph ligand *trans* to the methyl ligand in **1b** and **4**, this signal was assigned to P(2), which is *trans* to the methyl ligand in **2b**. Consequently, the other doublet at δ -4.6 was

(8) (a) Sakaki, S.; Ieki, M. *J. Am. Chem. Soc.* **1991**, *113*, 5063. (b) Sakaki, S.; Ieki, M. *J. Am. Chem. Soc.* **1993**, *115*, 2373. (c) Levy, C. J.; Puddephatt, R. J. *Organometallics* **1995**, *14*, 5019. (d) Pilcher, G.; Skinner, H. A. In *The Chemistry of the Metal–Carbon Bond*; Hartley, F. R., Patai, S., Eds.; Wiley: Chichester, U.K., 1982; Vol. 1, p 43. (9) Ozawa, F.; Hikida, T. *Organometallics* **1996**, *15*, 4501.

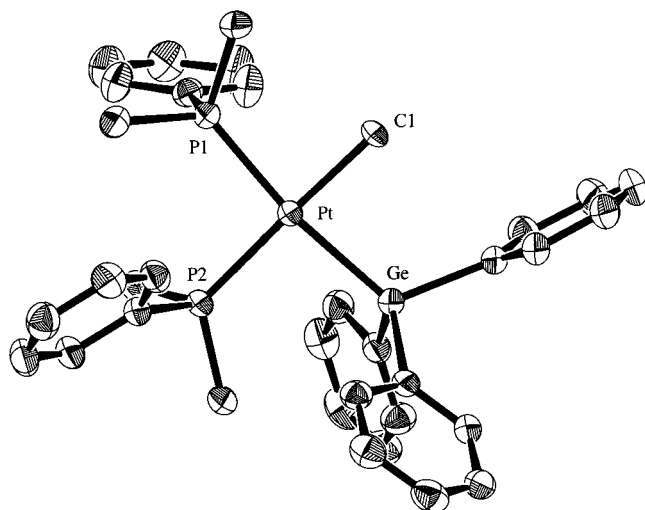
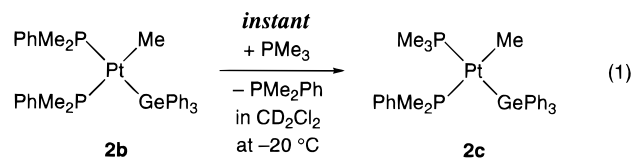


Figure 1. Molecular structure of *cis*-PtMe(GePh₃)(PMe₂-Ph)₂ (**2b**). Thermal ellipsoids are drawn at the 30% probability level. Selected bond distances (Å) and angles (deg): Pt–Ge = 2.4495(7), Pt–C(1) = 2.127(5), Pt–P(1) = 2.330(1), Pt–P(2) = 2.308(2); Ge–Pt–C(1) = 85.6(2), P(1)–Pt–P(2) = 94.28(5), Ge–Pt–P(2) = 93.41(4), P(1)–Pt–C(1) = 87.0(2), Ge–Pt–P(1) = 166.48(4), P(2)–Pt–C(1) = 178.2(2).

assigned to P(1) trans to the GePh₃ ligand. It is seen from Table 1 that the $^1J_{\text{Pt-P}(1)}$ value (1955 Hz) is somewhat smaller than the $^1J_{\text{Pt-P}(2)}$ value (1972 Hz). On the other hand, in the $^{31}\text{P}\{^1\text{H}\}$ NMR spectrum of methyl–silyl complex **1b**, the Pt–P coupling constants were much smaller at the trans position (P(1), 1330 Hz) than at the cis position (P(2), 2048 Hz) of the SiPh₃ ligand. Hence, the following order of trans influence was evidenced: SiPh₃ \gg GePh₃ > Me. This order is consistent with previous observations.¹⁰

X-ray Structure of 2b. Figure 1 shows the ORTEP drawing of **2b**. The platinum atom had a slightly distorted square planar geometry, and the sum of four angles about platinum was 360.3°. The Ge–Pt–P(2) angle (93.41(4)°) was significantly wider than the P(1)–Pt–C(1) angle (87.0(2)°), probably reflecting the steric bulkiness of the GePh₃ ligand. The Pt–P(1) bond (2.330(1) Å), which is situated trans to the GePh₃ ligand, was somewhat longer than the Pt–P(2) bond (2.308(2) Å) at the site trans to the methyl ligand, indicating that the germyl ligand has a greater trans influence than the methyl ligand. This result is consistent with the $^1J_{\text{Pt-P}}$ values of **2b**. However, reflecting the modest trans influence of the GePh₃ ligand as compared with the SiPh₃ ligand, the difference between the two Pt–P distances of **2b** (0.022 Å) was much smaller than that observed for *cis*-PtMe(SiPh₃)(PMe₂Ph)₂ (**1a**) (0.268 Å).⁴

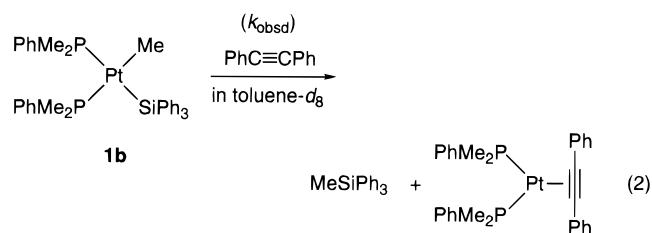
Reactivity toward Ligand Substitution. The NMR and X-ray diffraction data for **2b** indicated that the GePh₃ ligand possesses only a slightly higher trans influence than the methyl ligand. On the other hand, the following investigation demonstrated that the GePh₃ ligand has a much greater trans effect than the methyl ligand, comparable to that of the SiPh₃ ligand (eq 1).



Complex **2b** was treated with PMe₃ in CD₂Cl₂ at –20 °C, and the reaction system was examined by $^{31}\text{P}\{^1\text{H}\}$ NMR spectroscopy at –70 °C. On addition of 1 equiv of PMe₃ to the system, complex **2b** was selectively converted to the new methyl–germyl complex **2c** with liberation of 1 equiv of PMe₂Ph. Thus, as the reaction proceeded, the doublet at δ –4.1 due to the PMe₂Ph ligand trans to the GePh₃ ligand in **2b** (P(1)) instantly disappeared, to be replaced by a new doublet at δ –14.1 ($^2J_{\text{P-P}} = 20$ Hz, $^1J_{\text{Pt-P}} = 1906$ Hz), which was assignable to the PMe₃ ligand at the coordination site trans to the GePh₃ ligand. Simultaneously observed were a broad singlet of free PMe₂Ph (δ –44.9) and a doublet at δ –12.5 ($^2J_{\text{P-P}} = 20$ Hz, $^1J_{\text{Pt-P}} = 1960$ Hz). Since the latter signal exhibited almost the same chemical shift as the P(2) signal of the starting **2b** (δ –12.1), this doublet was assigned to the PMe₂Ph ligand trans to the methyl group. Therefore, we concluded that complex **2c** is PtMe(GePh₃)(PMe₃)(PMe₂Ph), in which PMe₃ and PMe₂Ph are oriented trans and cis toward the GePh₃ ligand, respectively, and the ligand substitution took place only at the coordination site trans to the GePh₃ ligand.

The site-selective ligand displacement with phosphine was also observed for methyl–silyl complexes **1a**^{4,9} and **1b**.¹¹ In these cases the ligand substitution proceeded instantly at –20 °C at the site trans to the SiPh₃ ligand. It was further confirmed that the phosphine ligand trans to the methyl ligand is inactive toward ligand substitution, even in the presence of an excess amount of added phosphine at room temperature.⁹

Kinetic Studies on Reductive Elimination. (a) *cis*-PtMe(SiPh₃)(PMe₂Ph)₂ (**1b**). The thermolysis reaction of **1b** was examined in toluene-*d*₈ in the presence of an excess amount of diphenylacetylene. The reaction gave MeSiPh₃ and Pt(PhC≡CPh)(PMe₂Ph)₂ as the reductive-elimination products in quantitative yields (eq 2). In the presence of 0.20 M (10 equiv/**1b**) of



diphenylacetylene at 30 °C, the reductive elimination proceeded by obeying the first-order rate law with respect to the concentration of **1b** over 70% conversion ($k_{\text{obsd}} = 2.2 \times 10^{-4} \text{ s}^{-1}$). The reaction was somewhat slower than the reductive elimination of *cis*-PtMe-

(10) Appleton, T. G.; Clark, H. C.; Manzer, L. E. *Coord. Chem. Rev.* **1973**, *10*, 335. Bresciani-Pahor, N.; Forcolin, M.; Marzilli, L. G.; Randaccio, L.; Summers, M. F.; Toscano, P. J. *Coord. Chem. Rev.* **1985**, *63*, 1.

(11) The reaction of **1b** with PMe₃ (1 equiv) in CD₂Cl₂ at –20 °C instantly formed PtMe(SiPh₃)(PMe₃)(PMe₂Ph), having the PMe₃ and PMe₂Ph ligands trans and cis to the SiPh₃ ligand, respectively. $^{31}\text{P}\{^1\text{H}\}$ NMR (–70 °C): δ –10.8 (d, $^1J_{\text{Pt-P}} = 2027$ Hz, $^2J_{\text{P-P}} = 22$ Hz), –12.5 (d, $^1J_{\text{Pt-P}} = 1306$ Hz, $^2J_{\text{P-P}} = 22$ Hz).

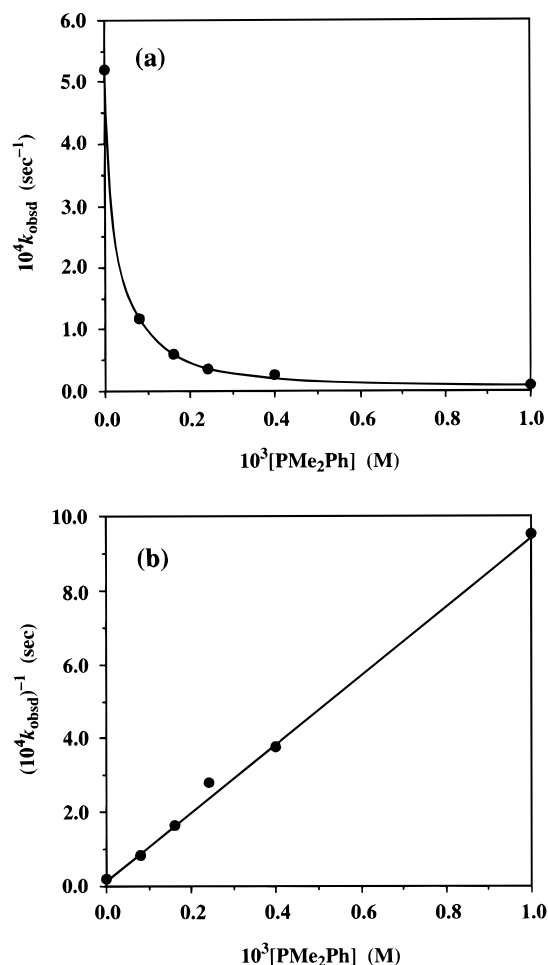


Figure 2. Effect of added PMe_2Ph on the reductive elimination of **1b** in toluene- d_8 in the presence of diphenylacetylene at 35 °C. Initial concentrations: **[1b]** = 0.020 M, **[PhC≡CPh]** = 0.20 M.

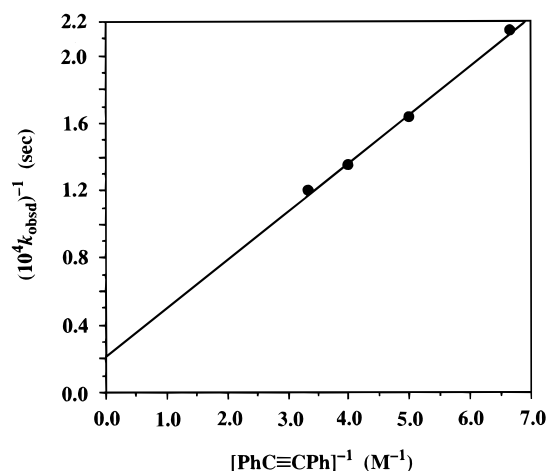


Figure 3. Effect of diphenylacetylene on the reductive elimination of **1b** in toluene- d_8 in the presence of added PMe_2Ph at 35 °C. Initial concentrations: **[1b]** = 0.020 M, **[PMe₂Ph]** = 1.6×10^{-4} M.

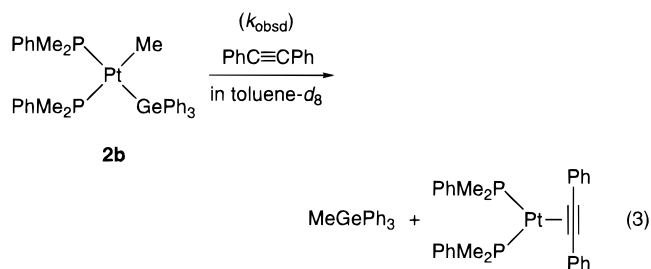
(SiPh_3)(PMePh_2)₂ (**1a**) under the same reaction conditions ($k_{\text{obsd}} = 5.0 \times 10^{-4} \text{ s}^{-1}$).

The reaction progress was severely hindered by addition of free PMe_2Ph to the system (Figure 2a). The plot of reciprocals of the rate constants ($1/k_{\text{obsd}}$) against the concentration of PMe_2Ph ($[\text{PMe}_2\text{Ph}]$) gave a straight

line (Figure 2b). On the other hand, the rate of reductive elimination increased as the concentration of diphenylacetylene increased and a linear correlation between $1/k_{\text{obsd}}$ and $1/[\text{PMe}_2\text{Ph}]$ values was observed.

These kinetic features are essentially the same as the previous observations for the reductive elimination of **1a**, except that the reaction of **1b** is almost entirely suppressed by addition of only a small amount of free PMe_2Ph (>5 mol %) to the system, while the reductive elimination of **1a** proceeds to some extent even in the presence of 1 equiv of added PMe_2Ph .

(b) *cis*-PtMe(GePh₃)(PMe₂Ph)₂ (2b**).** While the methyl-germyl complex **2b** also underwent reductive elimination cleanly in solution, the reaction progress was much slower than that of methyl-silyl complex **1b**. For example, the thermolysis of **2b** in toluene- d_8 in the presence of diphenylacetylene (0.20 M, 10 equiv) at 85 °C proceeded with the first-order rate constant $k_{\text{obsd}} = 1.4 \times 10^{-4} \text{ s}^{-1}$ to give MeGePh_3 and $\text{Pt}(\text{PhC}\equiv\text{CPh})(\text{PMe}_2\text{Ph})_2$ in quantitative yields (eq 3). Except for the higher



stability, kinetic features of the reductive elimination of **2b** were very similar to those of **1b**. Thus, the reaction was effectively retarded by addition of free PMe_2Ph to the system (Figure 4) and accelerated at a higher concentration of diphenylacetylene (Figure 5).

Reaction Mechanisms. The kinetic observations for **1b** and **2b** are consistent with the reductive-elimination process involving a prior displacement of one of the PMe_2Ph ligands with diphenylacetylene (Scheme 2). Considering the extremely high trans effects of SiPh_3 and GePh_3 ligands, which were suggested by the ligand substitution reactions of **1b** and **2b** with PMe_3 , the coordination of diphenylacetylene was assumed to take place selectively at the site trans to the EPh_3 ligand. This mechanism is almost identical with that previously proposed for **1a**, except for the absence of the direct reductive-elimination pathway from the *cis*- $\text{PtMe}(\text{EPh}_3)\text{-L}_2$ species. Assumptions of the ligand displacement to be a reversible process and of the rate-determining elimination of MeEPh_3 from the acetylene-coordinated species lead to the kinetic expressions in eqs 4 and 5, where $[\text{PtMe}(\text{EPh}_3)]_{\text{total}}$ is the sum of the concentrations of the *cis*- $\text{PtMe}(\text{EPh}_3)\text{L}_2$ complex and the acetylene-coordinated species at time t .

$$\frac{d[\text{MeEPh}_3]}{dt} = \frac{kK[\text{PhC}\equiv\text{CPh}]}{[\text{L}] + k[\text{PhC}\equiv\text{CPh}]} [\text{PtMe}(\text{EPh}_3)]_{\text{total}} \quad (4)$$

$$\frac{1}{k_{\text{obsd}}} = \frac{[\text{L}]}{kK[\text{PhC}\equiv\text{CPh}]} + \frac{1}{k} \quad (5)$$

These equations are consistent with the kinetic data for **1b** and **2b** represented in Figures 2 and 3 and

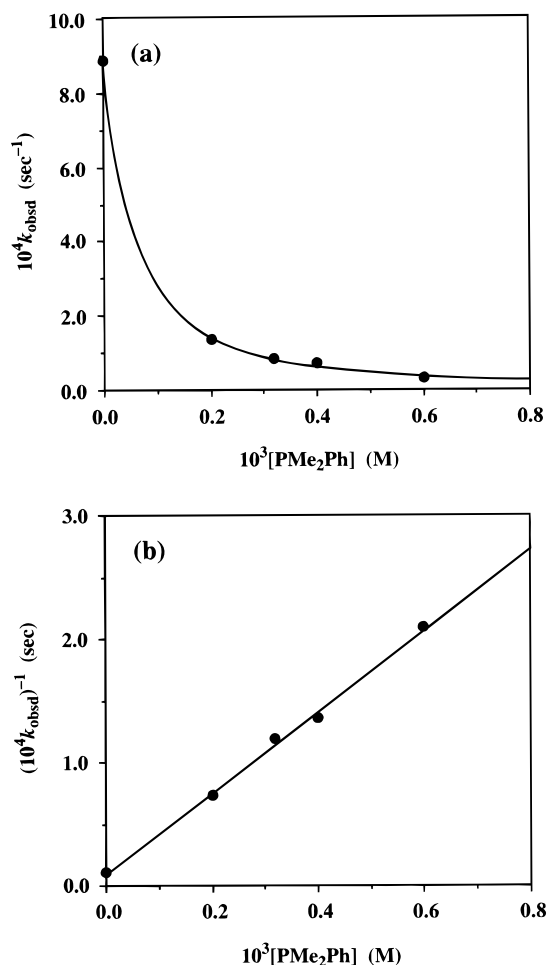


Figure 4. Effect of added PMe_2Ph on the reductive elimination of **2b** in toluene- d_8 in the presence of diphenylacetylene at 100 °C. Initial concentrations: $[\mathbf{2b}] = 0.020$ M, $[\text{PhC}\equiv\text{CPh}] = 0.20$ M.

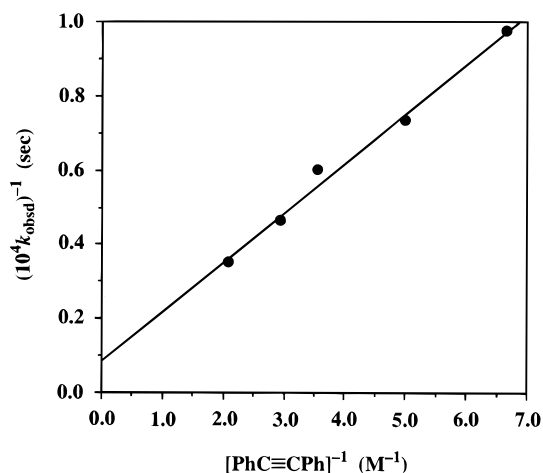


Figure 5. Effect of diphenylacetylene on the reductive elimination of **2b** in toluene- d_8 in the presence of added PMe_2Ph at 100 °C. Initial concentrations: $[\mathbf{2b}] = 0.20$ M, $[\text{PMe}_2\text{Ph}] = 2.0 \times 10^{-4}$ M.

Figures 4 and 5, respectively. For example, reciprocals of the values of intercepts in Figures 2 and 3, which correspond to the rate constants (k) for the reductive elimination of acetylene-coordinated methyl–silyl species at 35 °C, were in fair agreement with each other: $(4.5 \pm 0.05) \times 10^{-4} \text{ s}^{-1}$. On the other hand, the kK

Scheme 2

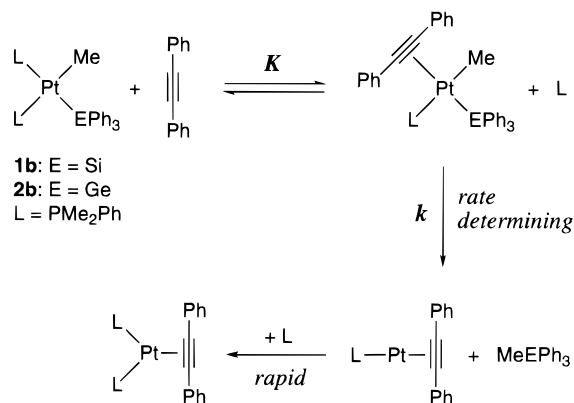


Table 2. Kinetic Parameters for the Reductive Elimination of **1b and **2b**^a**

1b (at 35 °C)	$k = 4.5 \times 10^{-4} \text{ s}^{-1}$	$(\Delta G^\ddagger = 22.8 \text{ kcal mol}^{-1})$
	$K = 1.2 \times 10^{-4}$	
	$\Delta H^\ddagger = 20.8 \text{ kcal mol}^{-1}$	$\Delta S^\ddagger = -6.8 \text{ eu}$
2b (at 100 °C)	$k = 1.1 \times 10^{-3} \text{ s}^{-1}$	$(\Delta G^\ddagger = 27.1 \text{ kcal mol}^{-1})$
	$K = 1.4 \times 10^{-4}$	
	$\Delta H^\ddagger = 28.5 \text{ kcal mol}^{-1}$	$\Delta S^\ddagger = 3.4 \text{ eu}$

^a The k and K values were calculated on the basis of the plots in Figures 2a and 3 for **1b** and Figures 4a and 5 for **2b**, respectively. Activation enthalpy and entropy were estimated from the Eyring plots of the rate constants measured at five different temperatures ranging from 20 to 45 °C for **1b** and from 80 to 100 °C for **2b**, respectively; the reactions were carried out in toluene- d_8 in the presence of 0.20 M diphenylacetylene.

values, which were calculated on the basis of the slopes in Figures 2 and 3, were in good agreement with each other: $(5.5 \pm 0.1) \times 10^{-8} \text{ s}^{-1}$. Similarly, the k and kK values for the reductive elimination of **2b** at 100 °C were successfully determined on the basis of the plots in Figures 4 and 5. The constants thus obtained are summarized in Table 2 together with the activation parameters estimated from Eyring plots.

The activation parameters listed in Table 2 indicate that the large difference in reactivities between **1b** and **2b** toward reductive elimination is mainly due to the difference in the activation enthalpies. Since **1b** and **2b** have almost the same structural features, the activation enthalpies may be dependent predominantly upon the Pt–E bond energies in the ground states and the bond energies of partially formed C–E bonds in the transition states. Generally, the C–Si bond is stronger than the C–Ge bond by 10–15 kcal mol^{-1} .¹² While the energy difference seems smaller for the incompletely formed C–Si and C–Ge bonds in the transition states, the order $D(\text{C–Si}) > D(\text{C–Ge})$ should be kept in the transition states as well. On the other hand, the data comparing the Pt–Si and Pt–Ge bond strengths are still lacking.⁸ However, experimental data for the related silyl and germyl complexes of late transition metals indicated the M–Si bond to be weaker than the M–Ge bond.¹³ Furthermore, a series of experiments regarding the metathesis reactions of *cis*-Pt(EMe_3)₂(dppe) or *cis*-

(12) For example, the mean bond dissociation enthalpies ($D(\text{E–C})$) in SiMe_4 and GeMe_4 are 76.5 and 61.7 kcal mol^{-1} , respectively.^{8d}

(13) Burnham, R. A.; Stobert, S. R. *J. Chem. Soc., Dalton Trans.* **1977**, 1489. Cardin, D. J.; Lappert, M. F.; Litzow, M. R.; Spalding, T. R. *J. Chem. Soc. A* **1971**, 2262. Spalding, T. R. *J. Organomet. Chem.* **1978**, 149, 371. Novak, I.; Huang, W.; Luo, L.; Huang, H. H.; Ang, H. G.; Zybail, C. E. *Organometallics* **1997**, 16, 1567.

PtCl(EMe₃)(dppe) with HE'Me₃ (E, E' = Si, Ge, Sn) suggested the following stability order of silyl, germyl, and stannyl complexes of platinum: E = Sn >> Ge > Si.¹⁴ Therefore, we are convinced that the higher reactivity of silyl complex **1b** than germyl complex **2b** toward reductive elimination is mainly due to the thermodynamic factors; that is, the Pt–Si bond is weaker than the Pt–Ge bond and the C–Si bond is stronger than the C–Ge bond.¹⁵

In conclusion, we have confirmed for the first time that methyl(silyl)platinum(II) is much more reactive than methyl(germyl)platinum(II) toward reductive elimination. Because the related dimethylplatinum(II) complexes are known to be inactive toward reductive elimination, the following order of reactivities is now clearly observed: C–Si > C–Ge >> C–C. The reactivity order is apparently inconsistent with the order of elements in the periodic table. The C–Si reductive elimination seems more thermodynamically favorable than the C–Ge reductive elimination and more kinetically favorable than C–C reductive elimination.

Experimental Section

General Procedure and Materials. All manipulations were carried out under a nitrogen atmosphere using conventional Schlenk techniques. Nitrogen gas was dried by passage through P₂O₅ (Merck, SICAPENT). NMR spectra were recorded on a JEOL JNM-A400 spectrometer (¹H NMR, 399.65 MHz; ¹³C NMR, 100.40 MHz; ³¹P NMR, 161.70 MHz). Chemical shifts are reported in δ (ppm), referenced to an internal SiMe₄ standard for ¹H and ¹³C NMR and to an external 85% H₃PO₄ standard for ³¹P NMR.

THF, Et₂O, benzene, and hexane were dried over sodium–benzophenone ketyl and distilled just before using. CH₂Cl₂ was dried over CaH₂ and distilled just before using. Benzene-*d*₆ and toluene-*d*₈ were dried over LiAlH₄, vacuum-transferred, and stored under a nitrogen atmosphere. PMe₂Ph was prepared by the reaction of MeMgBr with PCl₂Ph. *cis*-PtMe(SiPh₃)(PMe₂Ph)₂ (**1b**) was prepared as previously reported.⁹ All other compounds used in this study were obtained from commercial sources and used without purification.

Preparation of *trans*-PtCl(GePh₃)(PMe₂Ph)₂ (3**).** A mixture of *trans*-PtHCl(PMe₂Ph)₂ (750 mg, 1.2 mmol) and HGePh₃ (553 mg, 1.8 mmol) was heated at 90 °C without solvent. Upon heating with stirring, the mixture changed into a homogeneous solution and gradually turned orange with evolution of hydrogen gas. After 3 h, the mixture was cooled to –20 °C, washed with Et₂O (2 mL × 3), and dried under vacuum to give a white solid of the title compound (667 mg, 65%). This product was spectroscopically pure and was employed in the synthesis of **2b** without further purification. ¹H NMR (CDCl₃, 23 °C): δ 1.54 (virtual triplet, *J* = 3.4 Hz, ³*J*_{Pt–H} = 28.3 Hz, 12H, PCH₃), 7.4–7.6 (m, 25H, Ph). ³¹P{¹H} NMR (CDCl₃, 23 °C): δ –5.6 (s, ¹*J*_{Pt–P} = 2667 Hz).

Preparation of *cis*-PtMe(GePh₃)(PMe₂Ph)₂ (2b**).** To a solution of *trans*-PtCl(GePh₃)(PMe₂Ph)₂ (0.60 g, 0.74 mmol) in THF (10 mL) was added an ethereal solution of MeLi (Aldrich, low halide; 1.4 M, 1.1 mL, 1.5 mmol). The solution was stirred for 30 min at room temperature and then cooled to –20 °C.

Table 3. Crystal Data and Details of the Structure Determination for **2b**

formula	C ₃₅ H ₄₀ GeP ₂ Pt
fw	790.33
habit	prismatic
cryst size, mm	0.30 × 0.25 × 0.15
cryst syst	triclinic
space group	<i>P</i> $\bar{1}$ (No. 2)
<i>a</i> , Å	11.683(3)
<i>b</i> , Å	13.979(2)
<i>c</i> , Å	11.453(5)
α , deg	109.37(2)
β , deg	113.36(3)
γ , deg	82.88(2)
<i>V</i> , Å ³	1619.9(9)
<i>Z</i>	2
<i>d</i> _{calcd} , g cm ^{–3}	1.620
μ (Mo K α), cm ^{–1}	53.44
<i>F</i> (000)	780
radiation	Mo K α (λ = 0.710 69 Å)
monochromator	graphite
data collected	+ <i>h</i> , ± <i>k</i> , ± <i>l</i>
2 θ range, deg	4.0–54.9
scan type	ω –2 θ
$\Delta\omega$, deg	1.15 + 0.30 tan θ
scan speed, deg min ^{–1}	16, fixed
temp, K	293
linear decay, %	26.7
abs cor	empirical
min and max transmissn factors	0.535, 1.00
no. of rflns collected	7717
no. of unique rflns	7358 (<i>R</i> _{int} = 0.008)
no. of obsd rflns	6402 (<i>I</i> ≥ 3 σ (<i>I</i>))
no. of variables	352
<i>R</i>	0.041
<i>R</i> _w	0.052
goodness of fit	1.61
max $\Delta\sigma$ in final cycle	0.00
max and min peak, e Å ^{–3}	+1.00, –2.15 (near Pt)

Methanol (0.8 mL) was slowly added, and the mixture was concentrated to dryness by pumping. The resultant white solid was dissolved in benzene, filtered through a short Celite column, and then concentrated to dryness. The crude product was dissolved in CH₂Cl₂, and Et₂O was carefully layered on the CH₂Cl₂ solution. The solvent layers were allowed to stand at –70 °C overnight, giving colorless crystals of **2b** (0.38 g, 65%). ¹H NMR (CD₂Cl₂, –20 °C): δ 0.29 (dd, ³*J*_{P–H} = 11.7 and 6.3 Hz, ²*J*_{Pt–H} = 60.5 Hz, 3H, PtCH₃), 1.19 (d, ²*J*_{P–H} = 8.3 Hz, ³*J*_{Pt–H} = 21.5 Hz, 6H, PCH₃), 1.41 (d, ²*J*_{P–H} = 8.3 Hz, ³*J*_{Pt–H} = 21.5 Hz, 6H, PCH₃), 7.1–7.4 (m, 15H, Ph), 7.4–7.6 (m, 10H, Ph). ¹³C{¹H} NMR (CD₂Cl₂, –20 °C): δ –0.37 (dd, ²*J*_{P–C} = 83 and 7 Hz, ¹*J*_{Pt–C} = 486 Hz, PtCH₃), 14.2 (d, ¹*J*_{P–C} = 28 Hz, ²*J*_{Pt–C} = 26 Hz, PCH₃), 17.9 (dd, *J*_{P–C} = 30 and 3 Hz, ²*J*_{Pt–C} = 30 Hz, PCH₃), 127.0 (s, GePh), 127.6 (s, GePh), 128.7 (d, ³*J*_{P–C} = 8 Hz, PPh), 128.8 (d, ³*J*_{P–C} = 8 Hz, PPh), 130.2 (s, PPh), 131.6 (d, ²*J*_{P–C} = 12 Hz, ³*J*_{Pt–C} = 20 Hz, PPh), 131.8 (d, ²*J*_{P–C} = 12 Hz, ³*J*_{Pt–C} = 17 Hz, PPh), 137.0 (s, ³*J*_{Pt–C} = 13 Hz, GePh), 137.9 (d, ¹*J*_{P–C} = 41 Hz, ²*J*_{Pt–C} = 20 Hz, PPh), 140.2 (dd, ¹*J*_{P–C} = 43 and 3 Hz, ²*J*_{Pt–C} = 10 Hz, PPh), 148.8 (d, ³*J*_{P–C} = 10 Hz, ²*J*_{Pt–C} = 66 Hz, GePh). ³¹P{¹H} NMR (CD₂Cl₂, –20 °C): δ –12.2 (d, ²*J*_{P–P} = 19 Hz, ¹*J*_{Pt–P} = 1972 Hz), –4.6 (d, ²*J*_{P–P} = 19 Hz, ¹*J*_{Pt–P} = 1955 Hz). Anal. Calcd for C₃₅H₄₀P₂PtGe: C, 53.19; H, 5.10. Found: C, 52.75; H, 5.14.

X-ray Diffraction Study of *cis*-PtMe(GePh₃)(PMe₂Ph)₂ (2b**).** A single crystal of dimensions ca. 0.30 × 0.25 × 0.15 mm was sealed in a glass capillary tube. Intensity data were collected on a Rigaku AFC7R four-circle diffractometer. Unit cell dimensions were obtained from a least-squares treatment of the setting angles of 25 reflections in the range 39.60 ≤ 2 θ ≤ 39.91°. The cell dimensions suggested a triclinic cell, and a statistical analysis of intensity distribution indicated the space group *P* $\bar{1}$ (No. 2). Diffraction data were collected at 20 °C in the range 4.0 < 2 θ < 55° using the ω –2 θ scan technique at a scan rate of 16.0° min^{–1} in ω . Three standard reflections,

(14) Clemmit, A. F.; Glockling, F. *J. Chem. Soc. A* **1971**, 1164.

(15) After submission of this paper, the following decreasing order of Pt^{IV}–E bond energies was established on the basis of thermochemical experiments: E = Si > Ge > Sn. Levy, C. J.; Puddephatt, R. J. *J. Am. Chem. Soc.* **1997**, *119*, 10127; *Organometallics* **1997**, *16*, 4115. If this order is applied to the present Pt(II) systems, one must consider that the higher reactivity of **1b** compared to that of **2b** is mainly due to the stronger C–Si bond rather than C–Ge bond. The transition states may strongly resemble the reductive-elimination products.

monitored at every 150 reflection measurements, showed a linear decay in the intensity by 26.7%. The data were corrected for Lorentz and polarization effects, decay, and absorption (empirical, based on azimuthal scans of 3 reflections). Of the 7358 unique reflections measured, 6402 were classified as observed ($I > 3\sigma(I)$), and these were used for the solution and refinement of the structure.

All calculations were performed with the TEXSAN crystal structure analysis package provided by Rigaku Corp., Tokyo, Japan. The scattering factors were taken from ref 16. The structure was solved by heavy-atom Patterson methods (PATY) and expanded using Fourier techniques (DIRDIF92). The structure was refined by full-matrix least squares with anisotropic thermal parameters for all non-hydrogen atoms. In the final cycles of refinement, hydrogen atoms with isotropic temperature factors ($B_{\text{iso}} = 1.20 B_{\text{bonded atom}}$) were located at idealized positions ($d(\text{C-H}) = 0.95 \text{ \AA}$) and were included in calculations without refinement of their parameters. The function minimized in least squares was $\sum w(|F_o| - |F_c|)^2$ ($w = 1/[\sigma^2(F_o)]$). The final R index was 0.041 ($R_w = 0.052$, $S = 1.61$). $R = \sum ||F_o| - |F_c|| / \sum |F_o|$, and $R_w = [\sum w(|F_o| - |F_c|)^2 / \sum w|F_o|^2]^{1/2}$. $S = [\sum w(|F_o| - |F_c|)^2 / (N_o - N_p)]^{1/2}$, where N_o is the number of observed data and N_p is the number of parameters varied. Crystal data and details of data collection and refinement are summarized in Table 3. Additional information is available as Supporting Information.

Kinetic Studies. A typical procedure for the reductive elimination of **2b** is as follows. *cis*-PtMe(GePh₃)(PMe₂Ph)₂ (**2b**;

9.51 mg, 12.0 μmol) and diphenylacetylene (21.4 mg, 0.120 mmol) were placed in an NMR sample tube equipped with a rubber septum cap, and the system was replaced with nitrogen gas at room temperature. A solution of PMe₂Ph in toluene-*d*₈ (14.5 mM, 24.8 μL , 0.360 μmol) was added and then total volume of the solution was adjusted to 0.60 mL using neat toluene-*d*₈. The sample was placed in an NMR sample probe controlled to $100.0 \pm 0.1^\circ\text{C}$ and examined by ¹H NMR spectroscopy. The time course of the reductive elimination was followed by measuring the relative peak integration of the residual methyl signal of toluene-*d*₈ (δ 2.05) and the methyl signal of Pt(PhC \equiv CPh)(PMe₂Ph)₂ (δ 1.45) at intervals. The kinetic study for **1b** was similarly conducted. In this case, however, the time course of the reaction was followed by measuring the relative peak integration of the methyl signals of MeSiPh₃ (δ 0.74) and Me₂SiPh₂ (δ 0.45); the latter was used as an internal standard.

Acknowledgment. This work was supported by a Grant-in-Aid for Scientific Research on Priority Area "The Chemistry of Inter-element Linkage" (No. 09239105) from the Ministry of Education, Science, Sports and Culture of Japan.

Supporting Information Available: Details of the structure determination of **2b**, including a figure giving the atomic numbering scheme and tables of atomic coordinates, thermal parameters, and all bond distances and angles (9 pages). Ordering information is given on any current masthead page.

OM970841N

(16) Cromer, D. T.; Waber, J. T. *International Tables for X-ray Crystallography*; Kynoch Press: Birmingham, U.K., 1974; Vol. IV.